Sains Malaysiana 51(1)(2022): 315-328
http://doi.org/10.17576/jsm-2022-5101-26

AC Susceptibility and Electrical Properties of PbS added $Bi_{1.6}Pb_{0.4}Sr_2CaCu_2O_8$ Superconductor

(Kerentanan Arus Ulang Alik dan Sifat Elektrik Superkonduktor $Bi_{1.6}Pb_{0.4}Sr_2CaCu_2O_8$ dengan Penambahan PbS)

M.J. MASNITA, ROZIDAWATI AWANG & R. ABD-SHUKOR*

ABSTRACT

The $Bi_{1.6}Pb_{0.4}Sr_2CaCu_2O_8$ (Bi-2212) phase is an interesting superconductor. Although it's transition temperature is lower than $Bi_{1.6}Pb_{0.4}Sr_2Ca_2Cu_3O_{10}$ (Bi-2223), it has a better high field performance at low temperatures. This report is regarding the effects of lead sulfide on $Bi_{1.6}Pb_{0.4}Sr_2CaCu_2O_8$ superconductor. Samples of $Bi_{1.6}Pb_{0.4}Sr_2CaCu_2O_8(PbS)_x$ for x = 0.0 to 10.0 wt.% were prepared via the solid-state-reaction route. The Bi-2212 was the majority phase in all samples with x ≤ 1.0 wt.% showing more than 95%. Scanning electron micrographs showed increase in grain size as PbS content was increased. The x = 0 sample exhibited the highest $T_{c\text{-}zero}$ at 72 K and $T_{c\text{-}onset}$ 83 K. The imaginary part of the AC susceptibility showed that the peak temperature, T_p increased from 59 K for x = 0 to 66 K for x = 0.6 wt.% sample. This research showed that PbS increased the flux pinning of Bi-2212 for x ≤ 1.0 wt.% although the transition temperature was suppressed.

Keywords: AC susceptibility; lead sulfide; microstructure; X-ray diffraction

ABSTRAK

Fasa $Bi_{1.6}Pb_{0.4}Sr_2CaCu_2O_8$ (Bi-2212) adalah superkonduktor yang menarik. Walaupun suhu peralihannya lebih rendah daripada $Bi_{1.6}Pb_{0.4}Sr_2Ca_2Cu_3O_{10}$ (Bi-2223), ia mempunyai prestasi medan tinggi yang lebih baik pada suhu rendah. Penyelidikan ini adalah mengenai kesan plumbum sulfida terhadap superkonduktor $Bi_{1.6}Pb_{0.4}Sr_2CaCu_2O_8$. Sampel $Bi_{1.6}Pb_{0.4}Sr_2CaCu_2O_8(PbS)_x$ untuk x = 0.0 hingga 10.0 wt.% disediakan melalui tindak balas keadaan pepejal. Fasa Bi-2212 adalah majoriti dalam semua sampel dengan x ≤ 1.0 wt.% menunjukkan lebih daripada 95%. Mikrograf elektron imbasan tambahan menunjukkan peningkatan saiz butiran dengan peningkatan kandungan PbS. Sampel x = 0 menunjukkan $T_{c\text{-}sifar}$ tertinggi pada 72 K dan $T_{c\text{-}mula}$ tertinggi pada 83 K. Bahagian khayal kerentanan arus ulang alik χ" menunjukkan suhu puncak, T_p yang meningkat daripada 59 K untuk x = 0 hingga 66 K untuk sampel x = 0.6 %. Kajian ini menunjukkan bahawa PbS meningkatkan pengepinan fluks Bi-2212 untuk x ≤ 1.0 wt.% walaupun suhu genting menurun.

Kata kunci: Kerentanan arus ulang alik; mikrostruktur; pembelauan sinar-X; plumbum sulfida

INTRODUCTION

Among all classes of superconductors, the cuprate has great potential for application because of the high transition temperature, T_c and high critical magnetic field. The Bi-based cuprates consists of three phases: $Bi_2Sr_2Ca_{n-1}Cu_nO_y$ ($n = 1, 2, 3$) where n indicates the number of CuO_2 layers in a unit cell namely, $Bi_2Sr_2Ca_2Cu_3O_{10}$ (Bi-2223), $Bi_2Sr_2Ca_1Cu_2O_8$ (Bi-2212) and $Bi_2Sr_2CuO_6$ (Bi-2201). The Bi-based cuprate superconductors have some disadvantages including weak links, highly anisotropic and short coherence length which limits the performance. Due to the weak coupling between bismuth oxide layers, substitution with other elements for Bi^{3+} is necessary to improve the properties (Kaya et al. 2012). In order to improve critical current density, J_c defects were introduced in the crystalline structure and microstructure by addition or substitution of elements of compounds.

The Bi-2223 phase has been studied more compared with Bi-2212 due to its higher T_c. However, the Bi-2212 is more advantageous for high field applications between 4.2 and 20 K. Despite this fact, the Bi-2212 phase was not reported as widely as Bi-2223 (Marken et al. 2003, 1997). The Bi-2223 shows high J_c only in the tape form. Several techniques including powder-in-tube, dip-coating

and electrophoretic coating have been used to fabricate Bi-2212 with high J_c (Dietderich et al. 1990; Shimoyama et al. 1993; Tenbrink et al. 1993). Another advantage of the Bi-2212 phase is its suitability for round wires in high fields (Zhou et al. 2019). This phase has its own niche in superconductor applications.

The $YBa_2Ca_3O_7$ and Tl-based cuprates also showed improvement with substitution or addition with other elements or compounds (for e.g. Yusrianto et al. 2021). Semiconductors such as CdTe improved the flux pinning of the $Tl_2Ba_2CaCu_2O_8$ superconductor (Muhammad-Aizat & Abd-Shukor 2018). The substitution of metal sulfide into $YBa_2Ca_3O_7$ system showed less deteriorating effect on the T_c compared to metal oxide (Aguiar et al. 1996). PbS doping reduced voids in $YBa_2Cu_3O_7$ microstructure resulting in critical current densities improvement (Tyagi & Sharma 1994). PbS addition also showed an increase in shielding action against dc magnetic fields. It also increases the mechanical properties of $YBa_2Ca_3O_7$ by seven fold (Tyagi & Sharma 1994).

Metal sulfides have been added into Bi-2212. Some reports showed that metal sulfides stabilize the Bi-2212 phase and improved the superconducting transition temperature (Aguiar et al. 2000). The grain size of Bi-2212 was reduced when Cr_2S_3 was added (Farah-Elia et al. 2019). Addition of CuS nanoparticles into Bi-2223 introduces strong pinning centers which enhanced the flux pinning and transport properties (Loudhaief et al. 2020).

The effect of other metal sulfides on Bi-2212 is an interesting topic for investigation. In the present work, the effect of PbS on Bi-2212 was studied. Pb was chosen because it increased the superconducting volume fraction of the Bi-based materials (Dong et al. 2016). PbS has been chosen because metal sulfides have been shown to improve the flux pinning capabilities of the Bi-2212 phase. Hence, the combination of Pb and S addition in Bi-2212 phase is an interesting topic to study. PbS shows diamagnetic property with magnetic transition temperature 1127 °C (Pearce et al. 2006). The melting point of PbS is 1120 °C (Brebrick & Scanlon 1954) which is higher than the Bi-2212 formation temperature which is around 800-820 °C. In this work we investigated the effect of PbS on Bi-2212 on the phase, structure, microstructure, electrical transport properties and AC susceptibility.

EXPERIMENTAL DETAILS

The $Bi_{1.6}Pb_{0.4}Sr_2CaCu_2O_8$ were fabricated using Bi_2O_3, PbO, CaO, CuO and Sr_2CO_3 (≥99.9%) via the solid-state-reaction route. The powders were calcined for 24 h at 800 °C with two grinding cycles. PbS was added to the resultant powders with starting composition $Bi_{1.6}Pb_{0.4}Sr_2CaCu_2O_8(PbS)_x$ with x = 0, 0.6, 1.0, 3.0, 5.0 and 10.0 wt.% and pelletized (about 2.5 g each, 12.5 mm diameter and 2 mm thickness). The samples were heated at 820 °C in air for 24 h.

In order to identify the phase, we have used a Bruker D8 Advance x-ray diffractometer. A CuK_a source was used, and the scan was performed between 2θ = 0 and 60 °. We have used at least 10 peaks to determine the lattice parameters by least squares method. The volume fraction of the Bi-2212 and Bi-2201 phase was determined by using the formula:

$$\text{Bi-2212 \%} = \frac{\sum I_{2212}}{\sum I_{2212} + \sum I_{2201}} \times 100\%$$

$$\text{Bi-2201 \%} = \frac{\sum I_{2201}}{\sum I_{2212} + \sum I_{2201}} \times 100\%$$

where $\sum I_{2212}$ and $\sum I_{2201}$ the sum of intensities of Bi-2212 and Bi-2201 phase, respectively.

The microstructure was recorded using a Merlin Gemini field emission scanning electron microscope (FESEM). One hundred grains were used to estimate the average grain size using ImageJ software. An energy dispersive analyzer for Oxford Instruments was used to show the elemental composition of the samples.

The temperature dependent electrical resistance was measured using the four probe technique and silver paste was used as electrical contact. A Keithley 197 Autoranging Microvolt DMM and Keithley 220 Current Source with constant current from 1 to 100 mA was used. A CTI Cryogenics Model 22 closed cycle cryostat with temperature controller from Lake Shore Model 340 was used for low temperature measurements.

The complex AC susceptibility ($\chi = \chi' + i\chi''$) was measured using a susceptometer from Cryo Industry (REF-1808-AS). The magnetic field was 5 Oe and the frequency was 295 Hz. The critical current density at the peak temperature, T_p of the imaginary part of the susceptibility was determined by using Bean's model with $J_c(T_p) = H/w$, where H is the applied field and w is the cross-sectional dimension with the smallest width of the samples.

Results and Discussion

X-ray diffraction patterns showed that Bi-2212 phase was dominant in all samples (Figure 1). Bi-2201 peaks are marked with (*) and Ca_2PbO_4 with (#). The optimal heating temperature is vital for Bi-2212 phase formation which is shown through sharp and narrow XRD peaks (Darsono et al. 2016). Bi-2212 phase forms at least at 800 °C and higher temperatures will lead to other phases. The peak at $2\theta \sim 5.7$ ° corresponds to (002) of the Bi-2212 phase. The Bi-2212 XRD intensity peaks decreased with PbS addition from 3 to 10 wt.%. The Bi-2201 peak was not observed in the $x = 0$ sample. For $x \geq 0.6$ wt.%, the Ca_2PbO_4 peak was observed at $2\theta = 17$ °. The intensity for Ca_2PbO_4 peak increased with the addition of PbS. The Bi-2201 phase started to appear in the 5 wt.% PbS added samples. No PbS peaks were observed in any samples due to the small addition. In this study, all peaks from the Bi-2212 and Bi-2201 phases have been used to estimate the volume fraction (Yavuz et al. 2016). The Bi-2212 phase decreased with the addition of PbS. Higher PbS addition showed increase in Bi-2201 volume fraction and a decrease in the transition temperature. Most of the peaks can be indexed to the orthorhombic lattice unit cell Bi-2212. The lattice parameters for $x = 0$ was a = 5.367 Å, b = 5.410 Å and c = 30.827 Å. No systematic change in the lattice parameters were observed. This indicated that PbS did not affect the lattice parameters in any systematic way.

The microstructure of Bi-2212 with and without PbS was examined by FESEM. The $x = 0$ sample showed less voids and flaky plate-like structure while x = 0.6, 1.0, 3.0 and 10.0 wt.% showed smaller flaky plate-like and more voids. All samples showed close-packed microstructure and well-defined grain boundaries (Figure 2). PbS-added samples exhibited a higher porosity. In general, the average grain size increased with PbS content. The average grain size for x = 0, 0.6, 1.0, 3.0 and 10.0 wt.% samples were 1.93, 2.70, 2.30, 2.62 and 3.09 µm, respectively. The EDX spectra are exhibited in Figure 3(a)-3(e). All samples showed the presence of Bi:Sr:Ca:Cu:O with the approximate 2:2:1:2:8 ratio. Pb and S peaks were seen in the spectra of the added samples.

The electrical resistance curves showed metal-like normal state behavior except for the $x = 10$ wt.% sample which showed semiconducting behavior (Figure 4). The $x = 0$ sample showed the highest onset transition temperature, $T_{c\text{-onset}}$ and zero-resistance transition temperature, $T_{c\text{-zero}}$ which are 83 K and 72 K, respectively. Samples with PbS addition showed reduced $T_{c\text{-zero}}$. At x = 10 wt.%, $T_{c\text{-onset}}$ = 60 K while $T_{c\text{-zero}}$ = 45 K. The large transition width indicates the presence of other phases. The resistance decreased with broader width transition implying the presence of Bi-2201 phase together with Bi-2212 phase (Azhan et al. 2016). This observation also agreed with volume fraction from XRD analysis. The room temperature resistivity, $\rho_{300\ K}$ increased with PbS (Table 1). This showed that the impurity phase increased with increasing PbS which resulted in decrease of the transition temperature.

Figure 5 shows the normalized resistance and the derivative, dR/dT versus temperature. The first peak in dR/dT, (T_{p1}) indicates superconductivity within grains where the grain boundary remains in the normal state. The second peak T_{p2} observed in x =10 wt.% (Figure 5(f)) indicates the temperature where supercurrent flows between grains in which the grain boundaries are also superconducting. All samples showed $T_{p1} = T_{p2}$ except for x = 10 wt.%. The transition width ($T_{p1} = T_{p2}$) indicated the presence of impurities in the system (Sahoo et al. 2013). In this study, impurity phases were (Bi-2201 and Ca_2PbO_4) observed in the sample with higher PbS content from the XRD patterns.

The AC susceptibility ($\chi = \chi' + i\chi''$) curves are shown in Figure 6. The transition temperature, $T_{c\chi'}$ is indicated by the decrease in χ' which signals the onset of bulk superconductivity. The $x = 0$ sample showed the highest $T_{c\chi'}$ (81 K). In our experiment, no intrinsic peaks were observed in all samples because the low applied field was not large enough to fully penetrate the Bi-2212 grains. T_p shifted to the lower temperatures which indicated that the flux pinning energy was weakened (Figure 6). The addition of smaller amounts of PbS showed improvement in the flux pinning because T_p was shifted to the higher temperatures compared to the x= 0 sample. T_p for $x = 0$ sample was 59 K and the $x = 0.06$ sample showed T_p = 66 K. The x = 3 to 5 wt.% samples showed suppressed T_p (Table 1). $J_c(T_p)$ was between 19 and 31 A cm^{-2}. PbS addition in $Bi_2Sr_2CaCu_2O_8$ suppressed $T_{c\ onset}$, $T_{c\ zero}$ (Figure 7) and the critical current density. In comparison, nanosized CuS increases the current density and critical magnetic fields of Bi-2223 superconductor (Loudhaief et al. 2020). Nanosized PbO also increased the J_c of Bi-2223 superconductor tapes (Yahya & Abd-Shukor 2014).

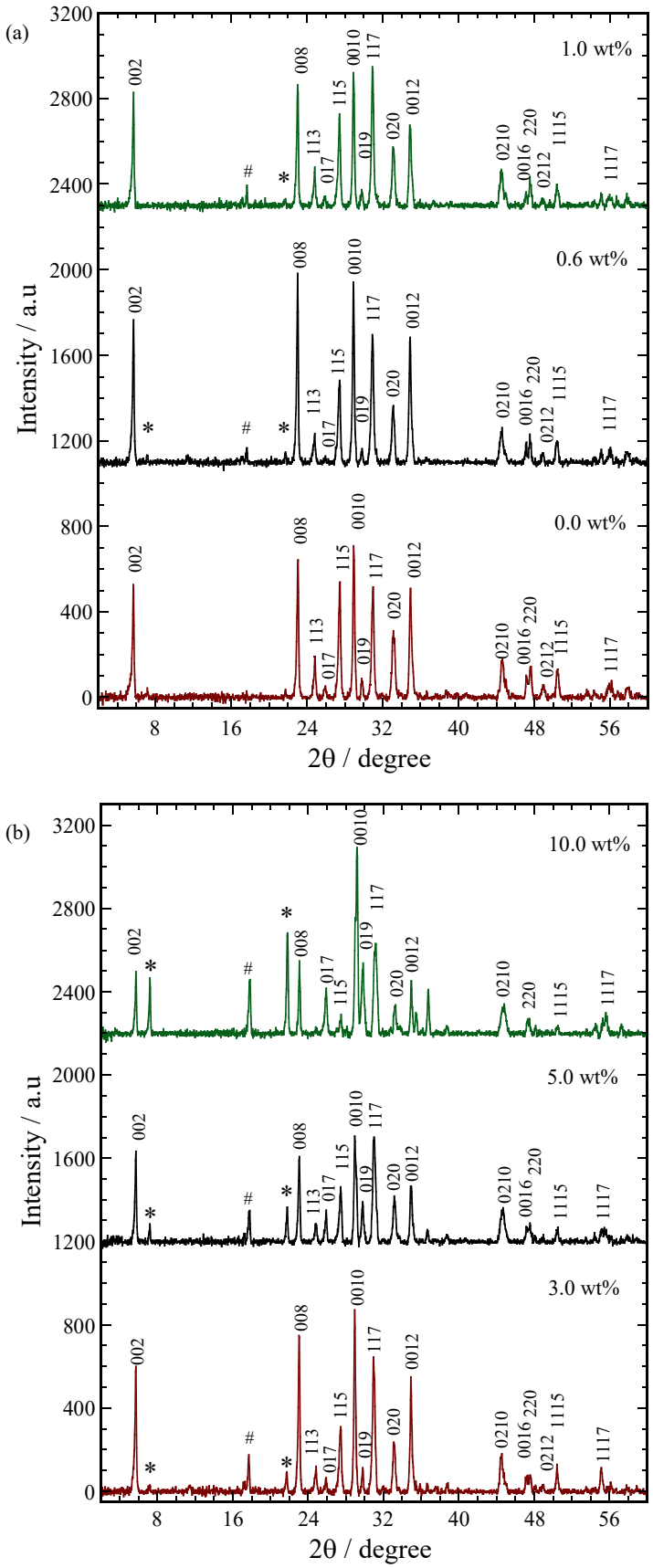

FIGURE 1. XRD patterns of $Bi_{1.6}Pb_{0.4}Sr_2CaCu_2O(PbS)_x$ for (a) $x = 0 – 1$ and (b) $x = 3 – 10$ wt.%. Peaks with (*) indicate Bi-2201 phase and (#) indicates Ca_2PbO_4

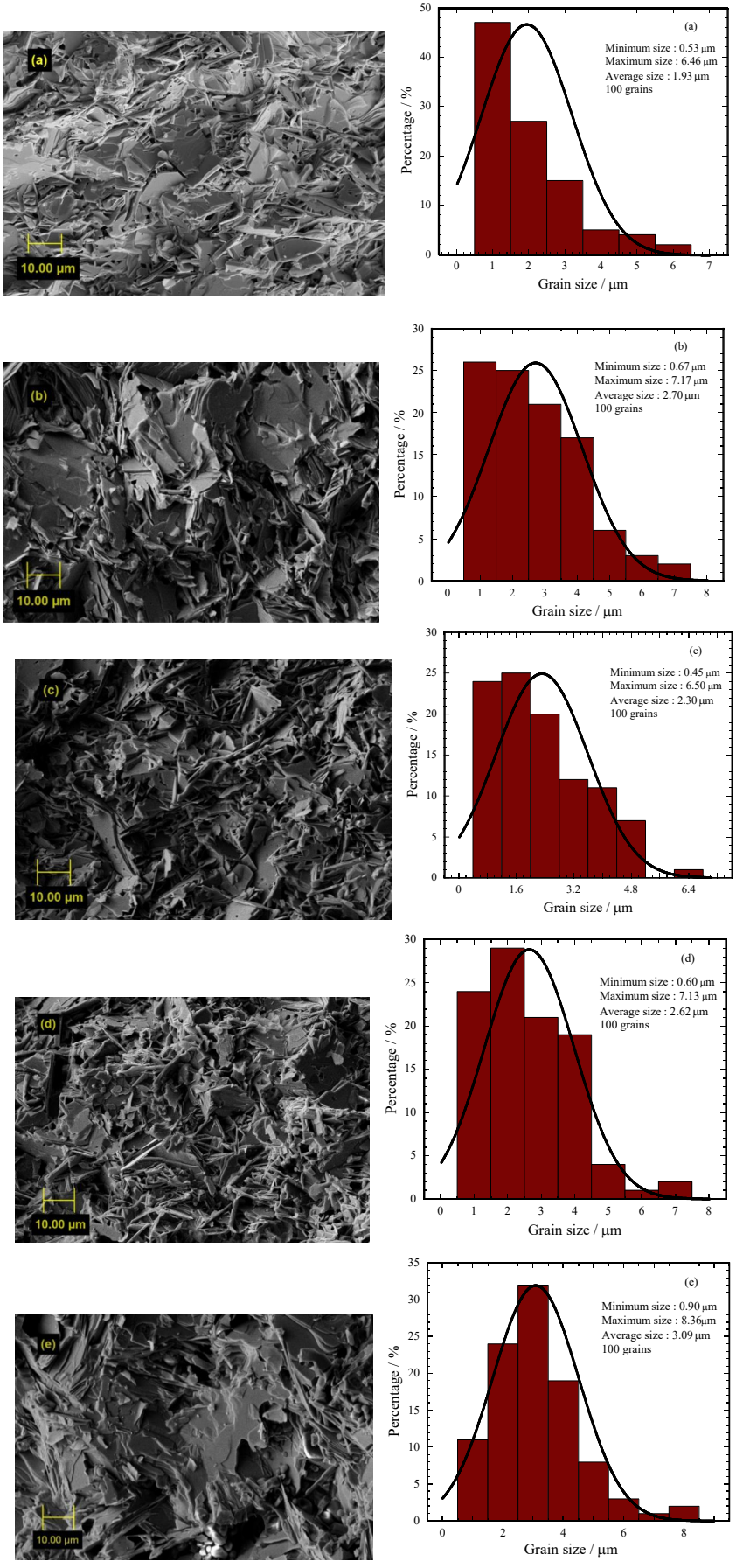

FIGURE 2. Scanning electron micrographs of $Bi_{1.6}Pb_{0.4}Sr_2CaCu_2O(PbS)_x$ for (a) x = 0, (b) x = 0.6, (c) x = 1, (d) x = 3 and (e) x = 10 wt.%. Histograms shows the average grain size of the samples

(a)

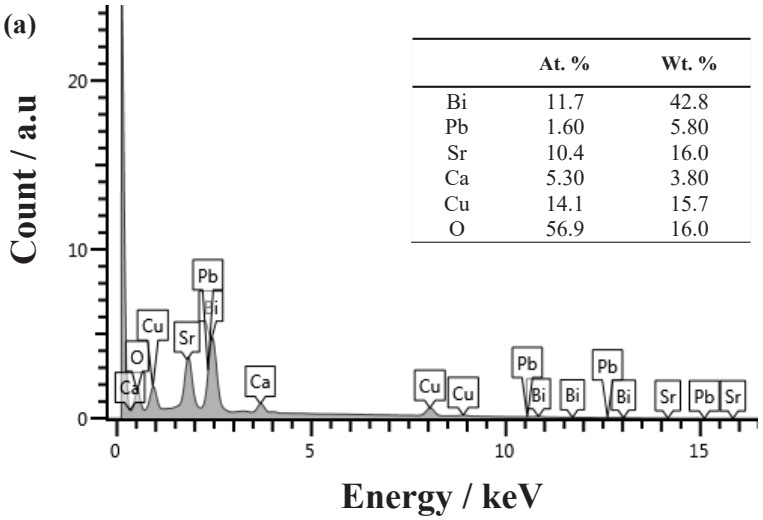

	At. %	Wt. %
Bi	11.7	42.8
Pb	1.60	5.80
Sr	10.4	16.0
Ca	5.30	3.80
Cu	14.1	15.7
O	56.9	16.0

(b)

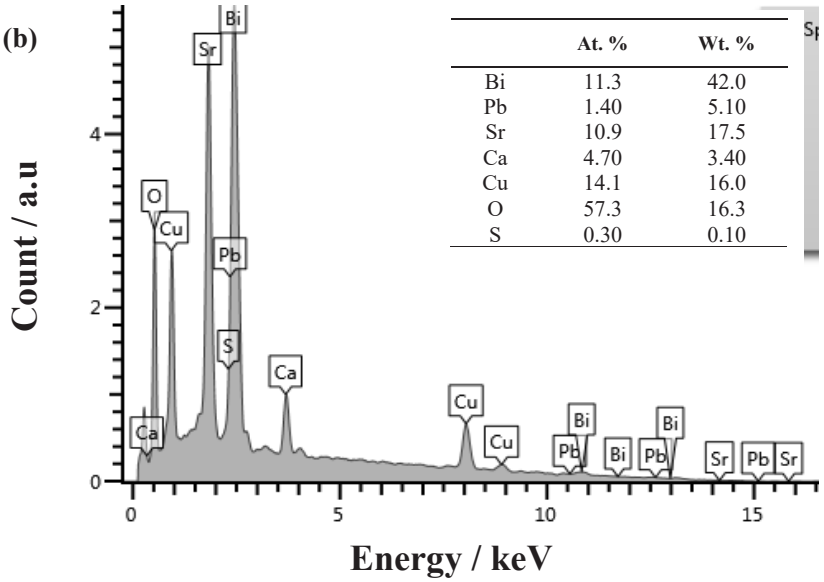

	At. %	Wt. %
Bi	11.3	42.0
Pb	1.40	5.10
Sr	10.9	17.5
Ca	4.70	3.40
Cu	14.1	16.0
O	57.3	16.3
S	0.30	0.10

(c)

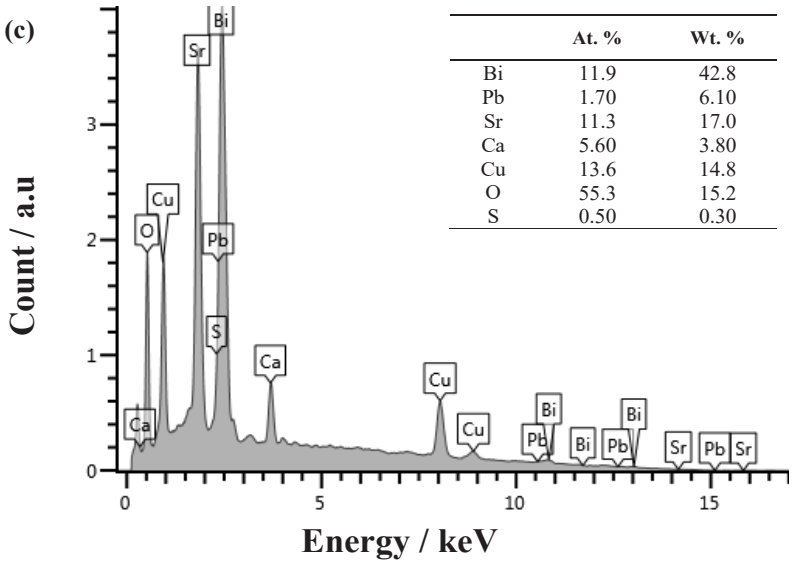

	At. %	Wt. %
Bi	11.9	42.8
Pb	1.70	6.10
Sr	11.3	17.0
Ca	5.60	3.80
Cu	13.6	14.8
O	55.3	15.2
S	0.50	0.30

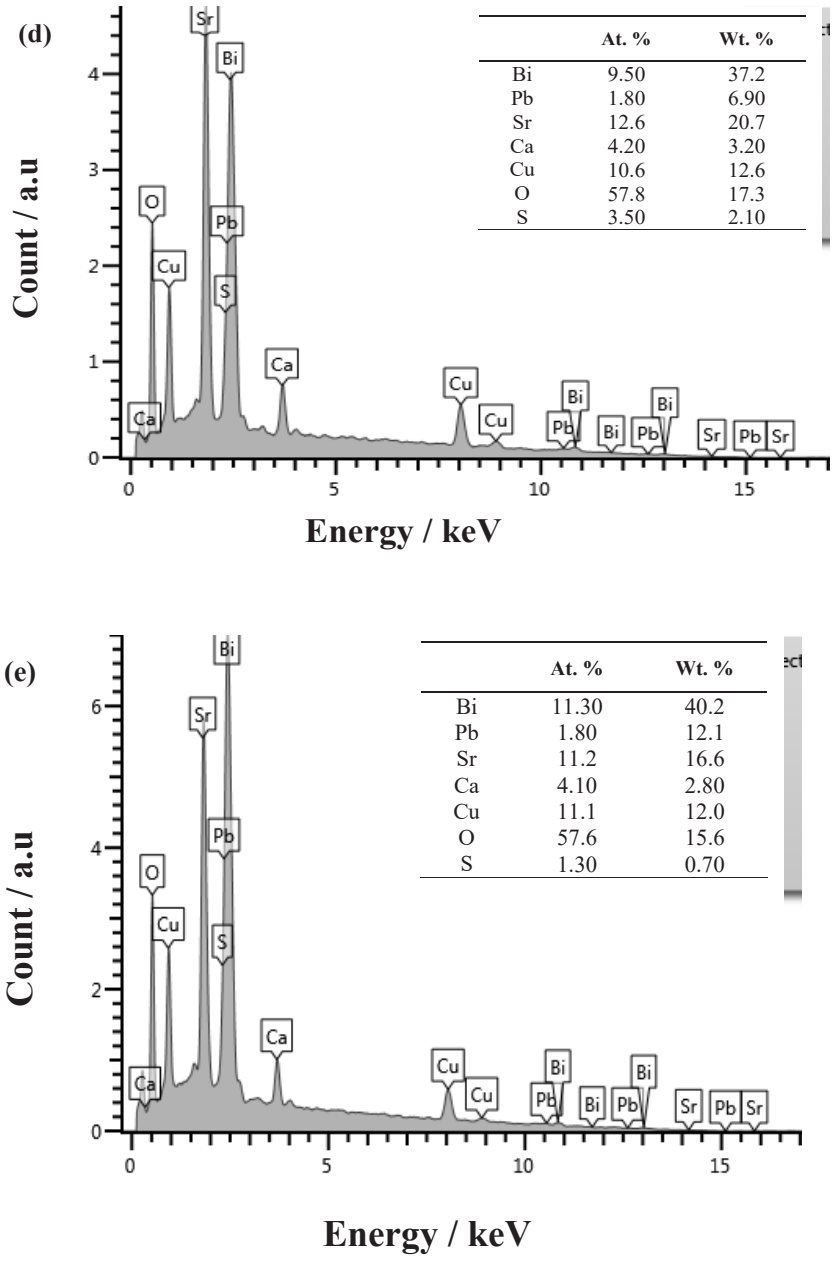

	At. %	Wt. %
Bi	9.50	37.2
Pb	1.80	6.90
Sr	12.6	20.7
Ca	4.20	3.20
Cu	10.6	12.6
O	57.8	17.3
S	3.50	2.10

	At. %	Wt. %
Bi	11.30	40.2
Pb	1.80	12.1
Sr	11.2	16.6
Ca	4.10	2.80
Cu	11.1	12.0
O	57.6	15.6
S	1.30	0.70

FIGURE 3. EDX spectra of $Bi_{1.6}Pb_{0.4}Sr_2CaCu_2O(PbS)_x$ for (a) $x = 0$, (b) $x = 0.6$, (c) $x = 1$, (d) $x = 3$ and (e) $x = 10$ wt.%. Inset shows the atomic and weight percent of the elements. All samples showed an approximate 2:2:1:2:8 for (Bi,Pb):Sr:Ca:Cu:O ratio

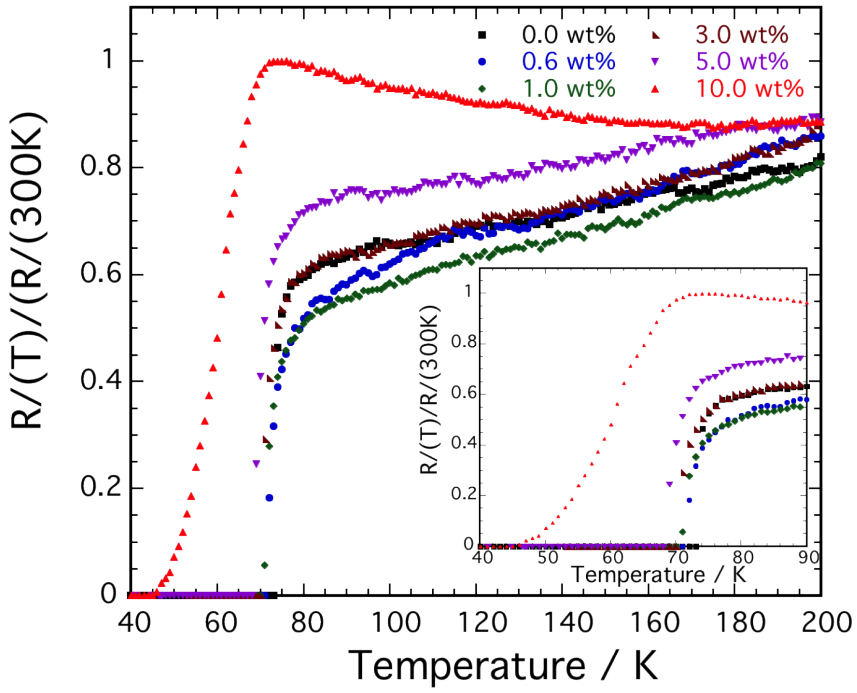

FIGURE 4. Electrical resistance versus temperature of $Bi_{1.6}Pb_{0.4}Sr_2CaCu_2O(PbS)_x$ for (a) x = 0 – 10 wt.%

TABLE 1. $T_{c\text{-onset}}$, $T_{c\text{-zero}}$, ΔT_c, $T_{c\chi'}$, T_p, $J_c(T_p)$, lattice parameters, unit cell volume of $Bi_{1.6}Pb_{0.4}Sr_2Ca_1Cu_2O(PbS)_x$ for x = 0, 0.6, 1, 3, 5 and 10 wt.%

x/ wt.%	$T_{c\text{-onset}}$ /K	$T_{c\text{-zero}}$ /K	ΔT_c /K	$T_{c\chi'}$ /K	T_p /K	J_c (T_p) / Acm^{-2}	r_{300K} /mΩcm	Grain size / μm	a /Å	b /Å	c /Å	V / Å^3	V_{2212}/%	V_{2201}/%
0	83	72	11	81	59	31.3	3.72	1.93	5.367	5.410	30.83	895.1	>97	<3
0.6	79	72	7	74	66	20.1	2.55	2.70	5.400	5.406	30.85	900.5	96	4
1.0	75	70	5	71	62	19.0	2.50	2.30	5.388	5.407	30.88	899.6	95	5
3.0	75	70	5	70	57	22.4	3.37	2.62	5.379	5.427	30.82	899.7	82	18
5.0	75	68	7	75	34	21.4	5.26	-	5.399	5.401	30.85	899.6	81	19
10.0	60	45	15	76	60	24.7	13.6	3.09	5.369	5.409	30.74	892.7	74	26

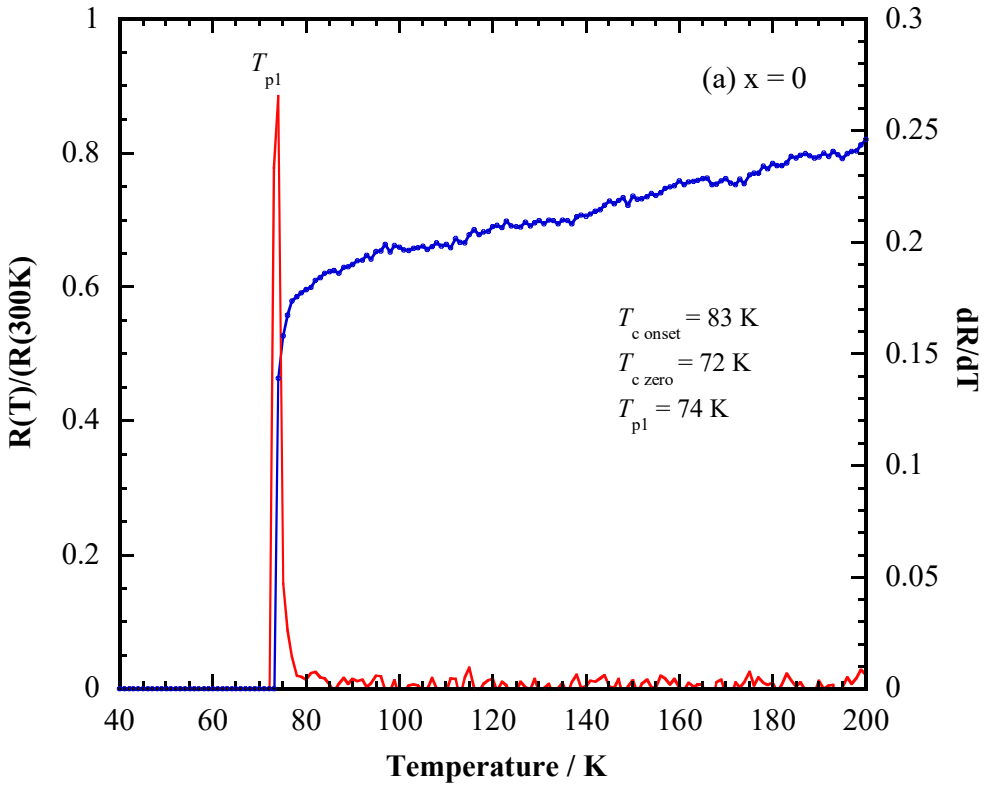
(a) x = 0
T_{p1}
$T_{c\ onset}$ = 83 K
$T_{c\ zero}$ = 72 K
T_{p1} = 74 K
R(T)/(R(300K)
dR/dT
Temperature / K

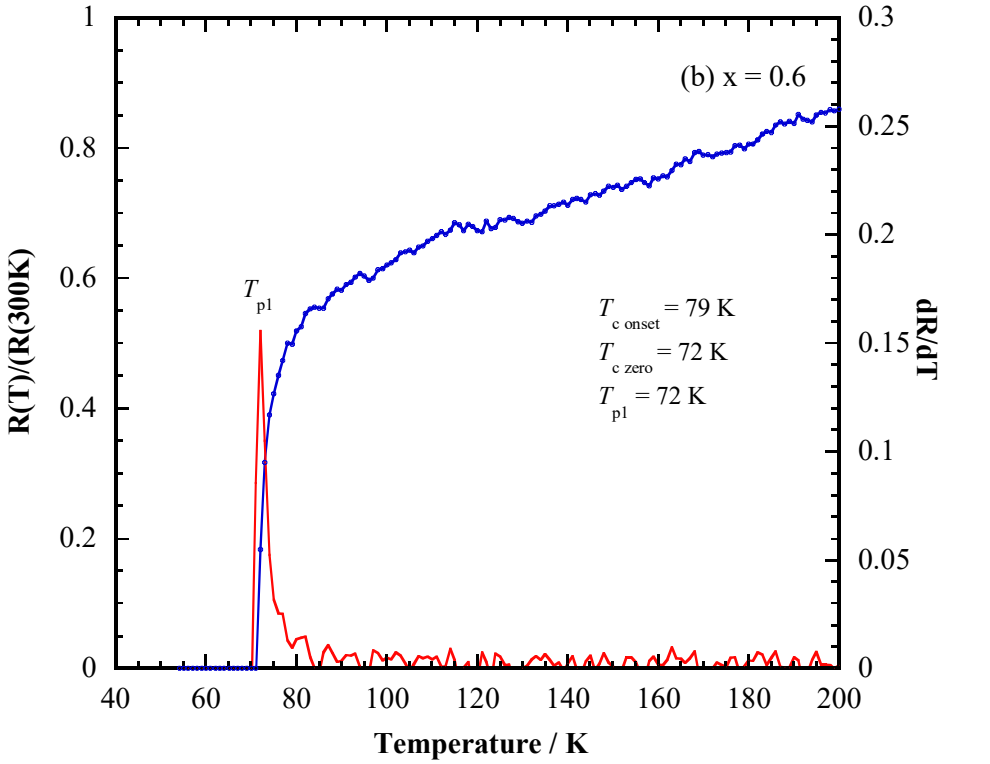
(b) x = 0.6
T_{p1}
$T_{c\ onset}$ = 79 K
$T_{c\ zero}$ = 72 K
T_{p1} = 72 K
R(T)/(R(300K)
dR/dT
Temperature / K

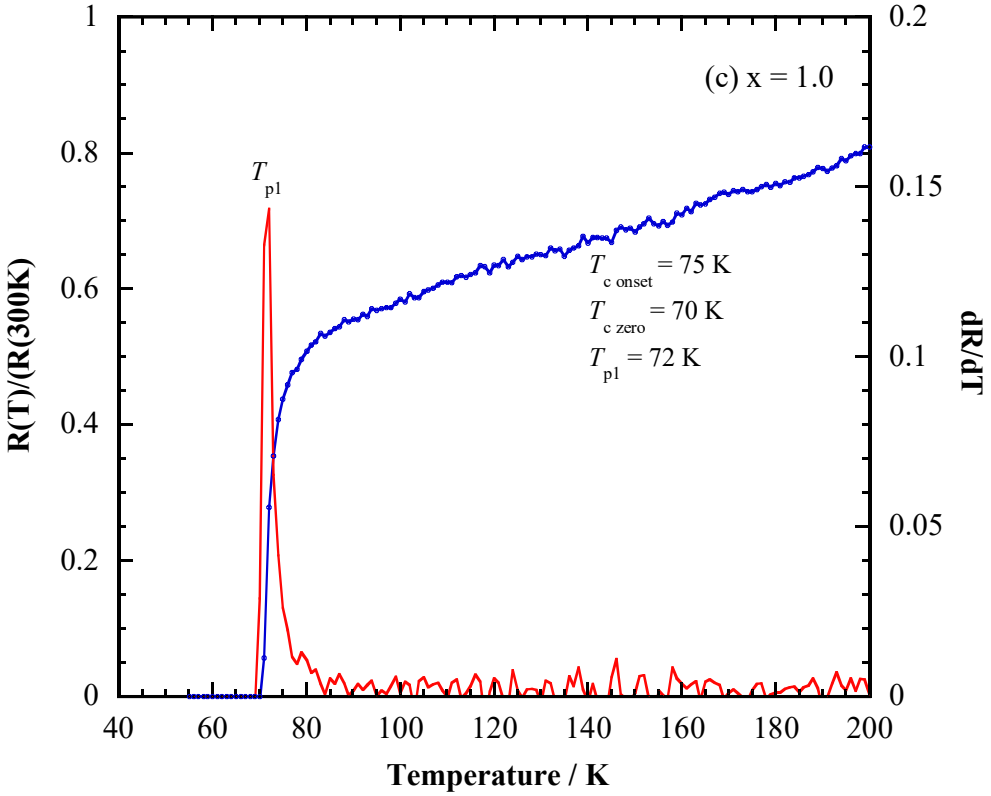
(c) x = 1.0
T_{p1}
$T_{c\ onset}$ = 75 K
$T_{c\ zero}$ = 70 K
T_{p1} = 72 K
R(T)/(R(300K))
dR/dT
Temperature / K

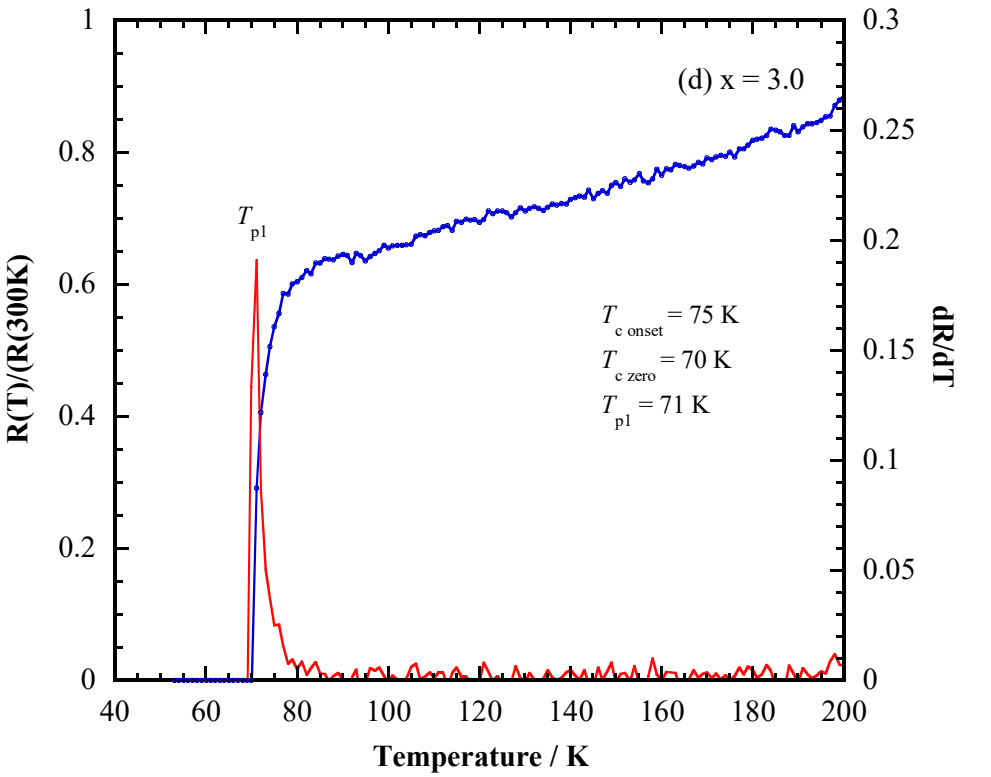
(d) x = 3.0
T_{p1}
$T_{c\ onset}$ = 75 K
$T_{c\ zero}$ = 70 K
T_{p1} = 71 K
R(T)/(R(300K))
dR/dT
Temperature / K

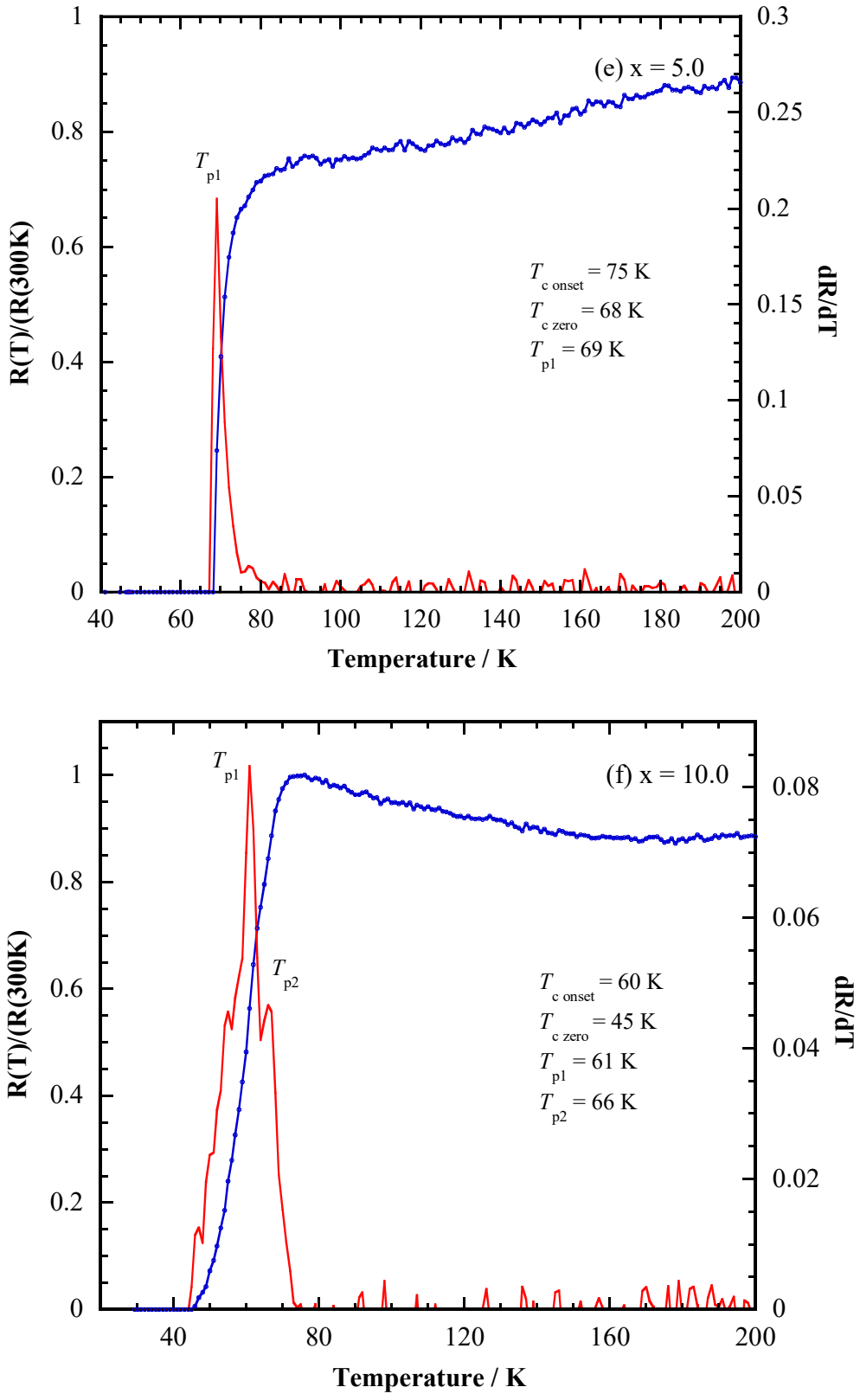

FIGURE 5. Normalized electrical resistance and the derivative, dR/dT with respect to temperature of $Bi_{1.6}Pb_{0.4}Sr_2CaCu_2O(PbS)_x$ for (a) x = 0, (b) x = 0.6, (c) x = 1, (d) x = 3 and (e) x = 10 wt.%

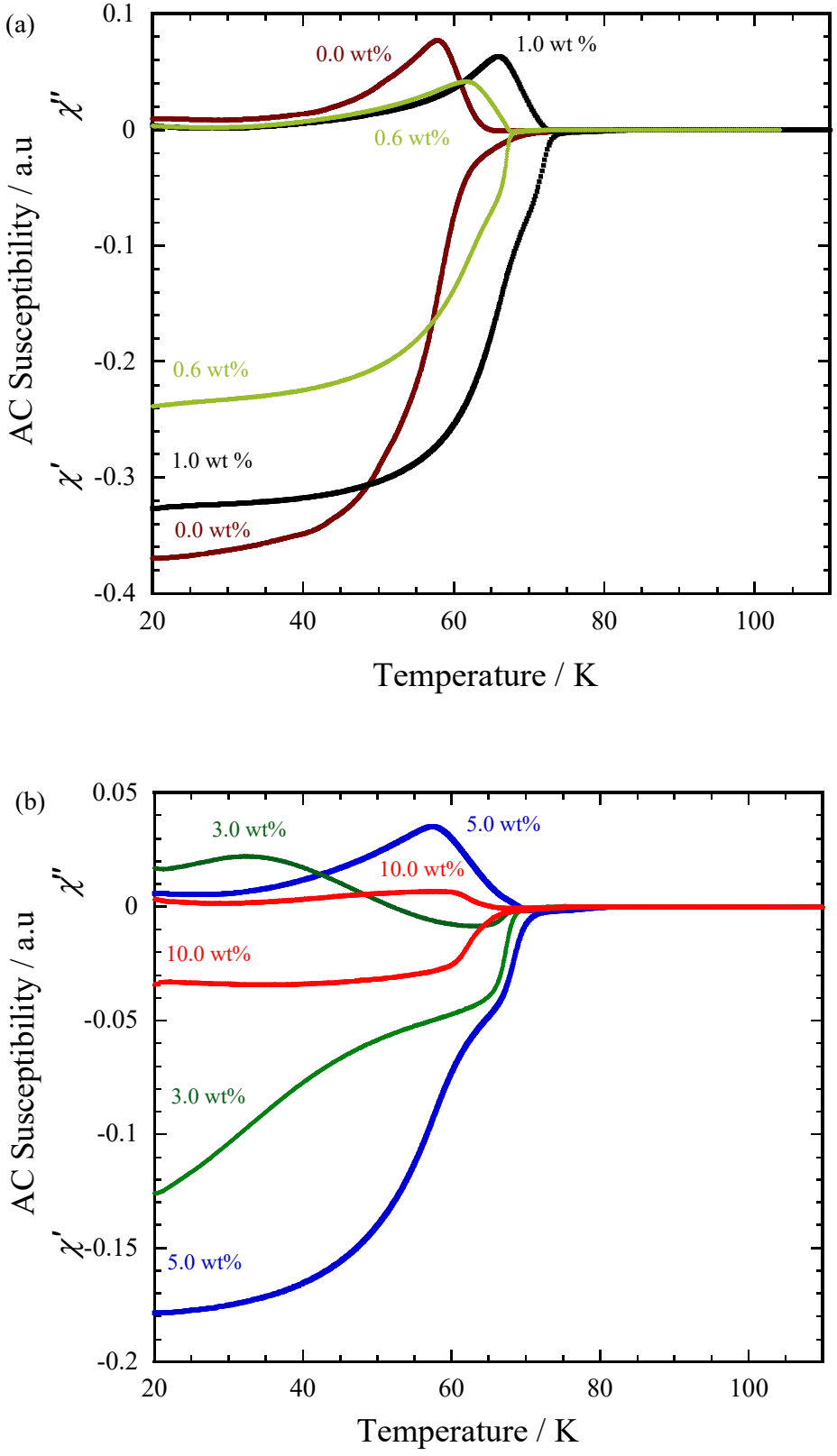

FIGURE 6. AC susceptibility ($\chi = \chi' + i\chi''$) versus temperature of $Bi_{1.6}Pb_{0.4}Sr_2Ca_1Cu_2O(PbS)_x$ for (a) $x = 0 - 1$ and (b) $x = 3 - 10$ wt.%

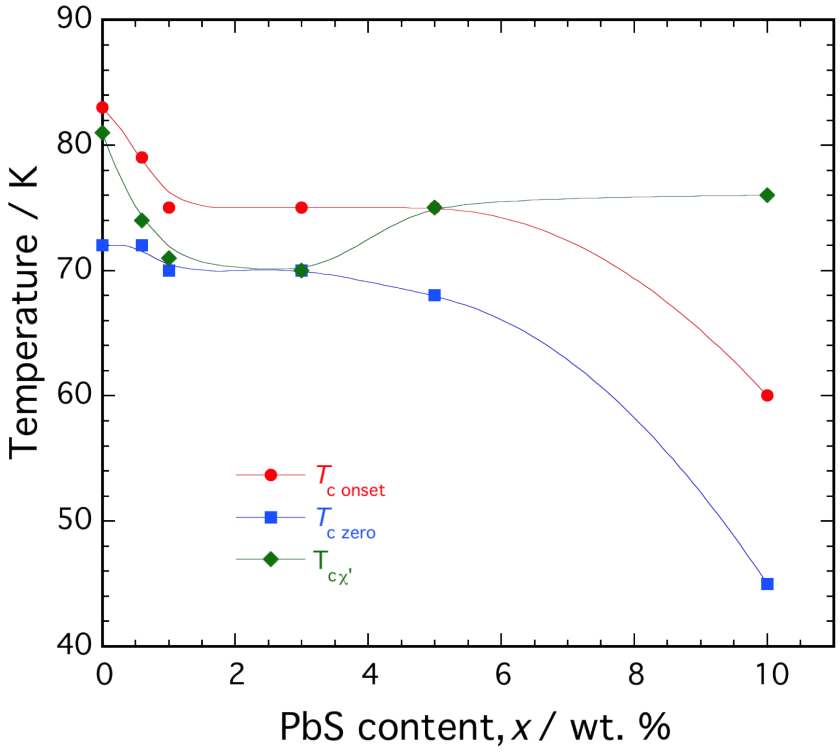

FIGURE 7. $T_{c\text{-onset}}$, $T_{c\text{-zero}}$ and $T_{c\chi'}$ versus x of $(Bi_{1.6}Pb_{0.4}Sr_2Ca_1Cu_2O)_x$ for $x = 0 – 10$ wt.%

CONCLUSION

The effects of diamagnetic PbS on $Bi_{1.6}Pb_{0.4}Sr_2CaCu_2O_8$ have been investigated. The transition temperature was reduced with PbS addition. Diamagnetic PbS reduced the superconducting properties of Bi-2212 phase. The increase in T_p for $x \leq 1.0$ wt.% showed that PbS can be used to enhance the flux pinning in Bi-2212 phase for low addition. It is also interesting to investigate the effect of nanosized PbS on the Bi-2212 and Bi-2223 phase. The effects of other nanosized metal sulfides with various magnetic properties on the Bi-2212 phase are interesting for further studies as well.

ACKNOWLEDGEMENTS

We thank the Ministry of Higher Education, Malaysia for the support under grant no. FRGS/1/2020/STG07/UKM/01/1.

REFERENCES

Aguiar, J.A., Lima, C.L.S., Yadava, Y.P., Tellez, D.L., Ferreira, J.M. & Montarroyos, E. 2000. EDX analysis, microstructureand magnetic properties of CuS doped Bi-2212 superconductors. *Physica C: Superconductivity* 341-348(Part 1): 593-596.

Aguiar, J.A., Ramos, A.S., Cabral, L.R., Barbosa, M.V., Awana, V.P.S., Ferreira, J.M., Pavão, A.C., Chavira, E. & Kurmaev, E.Z. 1996. Structural and superconducting properties of MS (M = Fe, Ni or Zn)-substituted $YBa_2Cu_3O_{7-\delta}$. *Journal of Physics: Condensed Matter* 8(49): 10545-10550.

Azhan, H., Hawa, J.S., Azura, C.M.N., Azman, K. & Syamsir, S.A. 2016. Structural and electrical properties of high and low Yb doped in Bi2223. *Jurnal Teknologi* 78(6-6): 7-12.

Brebrick, R.F. & Scanlon, W.W. 1954. Electrical properties and the solid-vapor equilibrium of lead sulfide. *Physical Review* 96(3): 598-602.

Darsono, N., Yoon, D-H. & Raju, K. 2016. Effects of the sintering conditions on the structural phase evolution and T_c of $Bi_{1.6}Pb_{0.4}Sr_2Ca_2Cu_3O_7$ prepared using the citrate sol-gel method. *Journal of Superconductivity and Novel Magnetism* 29(6): 1491-1497.

Dietderich, D.R., Ullmann, B., Freyhardt, H.C., Kase, J., Kumakura, H., Togano, K. & Maeda, H. 1990. Textured thick films of $Bi_2Sr_2Ca_1Cu_2O_x$. *Japanese Journal of Applied Physics* 29 (Part 2, No.7): L1100-L1103.

Dong, Y., Sun, A., Zhang, H., Zhang, M. & Xu, B. 2016. The effect of Sn substitution of Pb on microstructure and superconducting properties of Bi-Pb-Sr-Ca-Cu-O

superconductor. *Journal of Superconductivity and Novel Magnetism* 29(11): 2765-2769.

Farah-Elia, N.A.R., Ilhamsyah, A.B.P. & Abd-Shukor, R. 2019. Ferrimagnetic Cr_2S_3 effects on $(Bi_{1.6}Pb_{0.4})Sr_2CaCu_2O_6$ superconductor. *Journal of Materials Science: Materials in Electronics* 30(13): 12031-12035.

Kaya, C., Özçelik, B., Özkurt, B., Sotelo, A. & Madre, M.A. 2012. Effect of Ce substitution on structural and superconducting properties of Bi-2212 system. *Journal of Material Science: Materials in Electronics* 24(5): 1580-1586.

Loudhaief, N., Salem, M.B., Labiadh, H. & Zouaoui, M. 2020. Electrical properties and fluctuation induced conductivity studies of Bi-Based superconductors added by CuS nanoparticles synthesized through the aqueous route. *Materials Chemistry and Physics* 242: 122464.

Marken, K.R., Dai, W., Cowey, L., Ting, S. & Hong, S. 1997. Progress in BSCCO-2212/silver composite tape conductors. In *IEEE Transaction on Applied Superconductivity*. IEEE. 7(2): 2211-2214.

Marken, K.R., Miao, H., Meinesz, M., Czabaj, B. & Hong, S. 2003. BSCCO-2212 Conductor development at oxford superconducting technology. In *IEEE Transaction on Applied Superconductivity* 13(2): 3335-3338.

Muhammad-Aizat, K. & Abd-Shukor, R. 2018. Electrical properties and AC-susceptibility of CdTe added $Tl_2Ba_2CaCu_2O_{8-\delta}$ superconductor. *Sains Malaysiana* 47(7): 1579-1583.

Pearce, C.I., Pattrick, R.A. & Vaughan, D.J. 2006. Electrical and magnetic properties of sulfides. *Reviews in Mineralogy and Geochemistry* 61(1): 127-180.

Sahoo, M. & Behera, D. 2013. SCOPF analysis of $YBa_2Cu_3O_{7-\delta}$ + Cr_2O_3 superconductor composite. *Journal of Physics and Chemistry of Solids* 74(7): 950-956.

Shimoyama, J.I., Kadowaki, K., Kitaguchi, H., Kumakura, H., Togano, K., Maeda, H. & Nomura, K. 1993. Processing and fabrication of $Bi_2Sr_2CaCu_2O_y$/Ag tapes and small scale coils. *Applied Superconductivity* 1(1-2): 43-51.

Tenbrink, J., Wilhelm, M., Heine, K. & Krauth, H. 1993. Development of technical high-tc superconducting wires and tapes. In *IEEE Transaction on Applied Superconductivity* 3(1): 1123-1126.

Tyagi, A.K. & Sharma, T.P. 1994. Metallurgical reactions and enhanced magnetic field shielding in YBCO-PbS superconductor. *Materials Letters* 18(5-6): 341-348.

Yahya, N.A. & Abd-Shukor, R. 2014. Effects of nano-sized PbO on the transport critical current density of $(Bi_{1.6}Pb_{0.4}Sr_2Ca_2Cu_3O_{10})$/Ag tapes. *Ceramics International* 40(4): 5197-5200.

Yavuz, Ş., Bilgili, Ö. & Kocabaş, K. 2016. Effect of superconducting parameter of SnO_2 nanoparticles addition on (Bi, Pb)-2223 phase. *Journal of Materials Science: Materials in Electronics* 27(5): 4526-4533.

Yusrianto, E., Jannah, A.N. & Abd-Shukor, R. 2021. Phase formation and critical temperature of $(Tl_{0.5}Pb_{0.5})Sr_2Ca(Cu_{2-x}Cr_x)O_{7-\delta}$ (x = 0 - 0.100) superconductor. *Sains Malaysiana* 50(6): 1775-1786.

Zhou, X.X., Xue, F., Gou, X. & Shen, T.M. 2019. Statistical study of the void structure of Bi2212 multifilamentary superconductors wires and its effect on the critical current density. *Engineering Computations* 36(8): 2714-2725.

M.J. Masnita
Fakulti Sains Gunaan
Universiti Teknologi MARA
40450 Shah Alam, Selangor Darul Ehsan
Malaysia

M.J. Masnita, Rozidawati Awang & R. Abd-Shukor*
Department of Applied Physics
Universiti Kebangsaan Malaysia
43600 UKM Bangi, Selangor Darul Ehsan
Malaysia

*Corresponding author; email: ras@ukm.edu.my

Received: 9 March 2021
Accepted: 22 April 2021